ELSEVIER

Journal of Photochemistry and Photobiology A: Chemistry 137 (2000) 105–113

Journal of Photochemistry and Photobiology A:Chemistry

www.elsevier.nl/locate/jphotochem

Photophysical characteristics of two 4,6-disubistituted-3-cyanopyridin-2(1H)-thiones in various solvents

Maged A. El-Kemary [a,*], Mohamed E. El-Khouly [b], Osamu Ito [b]

[a] *Chemistry Department, Faculty of Education, Tanta University, Kafr El-Sheikh, Egypt*
[b] *Institute for Chemical Reaction Science, Tohoku University, Katahira, Aoba-ku, Sendai 980-8577, Japan*

Received 10 May 2000; received in revised form 31 July 2000; accepted 2 August 2000

Abstract

Photophysical and photochemical properties for 4,6-diphenyl-3-cyanopyridin-2(1H) thione (CPPT) and 4-phenyl-6-toly-3-cyanopyridin-2(1H)-thione (CMPT) have been investigated by various spectroscopic methods including transient absorption. With changing the solvent polarity, CPPT and CMPT exhibited the thione-thiol tautomeric equilibria. Laser flash photolysis studies in polar solvents and protic solvents have revealed that triplet state formation was predominantly observed by the thione tautomer, which was supported by the characteristic self-quenching in the rate constants of (2.99–5.68) $\times$ 10^9 dm^3 mol^{-1}. In nonopolar and less polar solvents, on the other hand, the thio radical was observed by photoinduced homolytic S–H bond cleavage of the thiol form. Absorption and fluorescence spectra indicate the considerable shifts with the solvent polarity in each form in addition to the equilibria. From the fluorescence lifetimes, the tautomeric forms can also be discriminated.

Keywords: Thione; Triplet state; Thio radical; Self-quenching; Fluorescence lifetime

1. Introduction

Pyridinethiones are a family of compounds that have been studied extensively [1–11] due to their application as biologically active compounds. They show antifungal, antibacterial, and anticancer properties [12–15] and were recently shown to cause DNA photodamage [16,17] and to induce photooxidation of purines [18].

Pyridinethiones are fundamentally tautomeric systems [1,19,20]. Several investigations showed that the position of this tautomeric equilibrium is influenced by the nature of environments [21–23]. Tautomerism of heteroaromatic compounds is thought to play a significant role in a number of biochemical processes such as proton transport, enzymatic catalysis, and spontaneous or induced mutagenesis [24–28].

In the present paper, we have investigated the photophysical and photochemical properties and reactivities of 4,6-diphenyl-3-cyanopyridin-2(1H)-thione (CPPT) and 4 phenyl-6-toly-3-cyanopyridin-2(1H)-thione (CMPT), which are in tautomeic equlibria in their thiol forms as shown in Scheme 1.

Steady-state and time-resolved absorption and fluorescence spectroscopies were employed to investigate the photochemical properties of these molecules in various solvents.

2. Experimental

2.1. Materials

4,6-Disubstituted-3-cyanopyridin-2(1H)-thiones were synthesized according to the procedure described in the literature [23,29] and were purified by recrystallization from ethanol. Disulfide of CPPT was prepared from the corresponding thione, through oxidation with equimolar amounts of H_2O_2 in ethanol [30] at room temperature. The purity of the compounds was checked by melting point and single spot on TLC.

All solvents used were analytical or spectroscopic-grade of highest available purity and supplied by Merck, BDH or Aldrich.

2.2. Apparatus and methods

The absorption and fluorescence spectra were recorded on a Shimadzu 240 UV–VIS spectrophotometer and a Shimadzu RF-540 spectrofluorometer, respectively. Fluorescence quantum yields were measured in various solvents relative to 7-amino-4-methylcoumarin (Φ_f = 0.79 in ethanol) [31], introducing the usual corrections for the instrumental spectral response and the solvent refractive index. All quantum yields obtained are the average of three

* Corresponding author.

1010-6030/00/$ – see front matter
PII: S1010-6030(00)00359-2

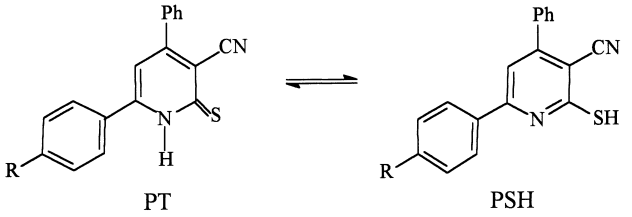

CPPT: R = H
CMPT: R = CH_3

Scheme 1.

independent measurements. The maximum absorbance was less than 0.1 in order to minimize errors due to inner filter effects.

The fluorescence lifetimes were measured with time-correlated single photon counting fluorimeter (Edinburgh Instruments, Model OB900); the half width of the instrument response was 1.0 ns.

Laser flash photolysis apparatus was a standard design with Nd:YAG laser of 6 ns duration [32]. Solution was photolyzed with FHG light (266 nm). The time profiles were followed by a photomultiplier system in the visible region. The laser photolysis was performed for deaerated and O_2-saturated solutions obtained by Ar and O_2 gas bubbling, respectively, in a rectangular quartz cell with a 10 mm optical path at 23°C.

Steady-state photolysis was carried out with a Xe-Hg lamp (150 W); the wavelength region of light was selected by using cut-off filters.

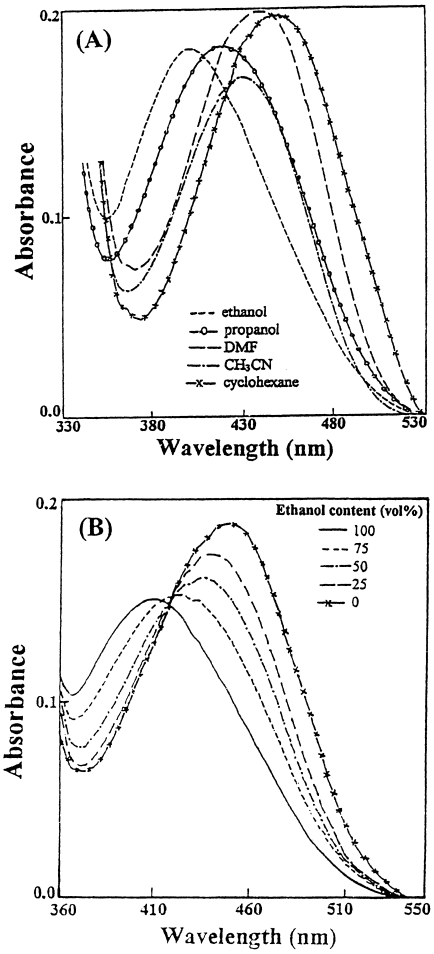

Fig. 1. (A) Absorption spectra of CMPT (4×10^{-5} M) in various solvents with 1.0 cm of optical path and (B) absorption spectra of CPPT in ethanol-CCl_4 mixture.

3. Results and discussion

3.1. Steady-state absorption and fluorescence studies

The absorption spectra of CMPT in various solvents are shown in Fig. 1A. In polar protic ethanol, the shortest absorption maximum (λ_{max}) was observed at 400 nm, while the longest λ_{max} was observed at 448 nm in non polar cyclohexane. In polar aprotic solvents such as acetonitrile and dimethylformamide, the λ_{max} stays in the intermediate region. A similar tendency was observed for CPPT. The λ_{max} values are summarized in Table 1.

Table 1
Spectroscopic data of CPPT and CMPT in various solvents at 298 K

Solvent	CPPT			CMPT		
	λ^{A}_{max} (nm)	λ^{F}_{max} (nm)	Δv (10^3 cm^{-1})	λ^{A}_{max} (nm)	λ^{F}_{max} (nm)	Δv (10^3 cm^{-1})
Ethanol	407	465	3.06	400	462	3.35
Propanol	431	493	2.92	418	490	3.50
Butanol	441	506	2.92	430	503	3.37
Acetonitrile	434	495	2.84	430	488	2.77
DMF[a]	439	505	2.98	438	502	2.91
Ethyl acetate	430	502	3.33	441	522	3.51
Diethyl ether	451	518	2.86	440	524	3.65
Dioxane	446	512	2.89	442	506	2.86
CCl_4	450	510	2.61	446	508	2.73
Cyclohexane[b]	452	510	2.51	488	504	2.48

[a] Dimethylformamide.
[b] 1% dioxane solution of cyclohexane due to very low solubility in cyclohexane.

The steady-state absorption spectra of CPPT in ethanol-CCl_4 solvent mixtures are shown in Fig. 1B. A single broad band at 407 nm in pure ethanol shifts to a longer wavelength with increasing content of aprotic, nonpolar solvent CCl_4 in ethanol, and λ_{max} shifts up to 450 nm in pure CCl_4. An isosbestic point is located at about 428 nm, suggesting that two equilibrium mixtures are responsible for these spectral changes. This can be understood in terms of tautomeric equilibrium between thione-forms (PT) and thiol-forms (PSH), due to the migration of the hydrogen atom between nitrogen and sulfur atoms according to Scheme 1 [33,34]. Since the λ_{max} of each component seems to be quite sensitive to the solvent polarity as shown in Fig. 1A (or Table 1), the λ_{max} shifts gradually with the change of the composition of ethanol-CCl_4. Some specific solute-solvent interaction such as hydrogen bonding may also play role in the spectral shift.

Fig. 2A displays the relative shift of the absorption and fluorescence maxima, Δv, for CPPT versus the mole fraction of ethanol in CCl_4. As shown below ethanol shows deviation from linearity due to intramolecular hydrogen bonding formation with solute. It can be observed that the relative shift of the absorption spectra with solvent composition is parallel to that of the fluorescence spectra, indicating that similar prototropic equilibria occurs in the ground and singlet excited states.

A plot of the relative fluorescence shift, v_f, versus the relative absorption shift, v_a, for CPPT in mixed ethanol/CCl_4 solvents with different compositions is shown in Fig. 2B. A good linear straight line with slope equal to 0.83 and correlation coefficients equal to 0.997 is obtained, supporting our conclusion that similar prototropic equilibria occurs in the ground and excited states. In all cases, a linear Beer–Lambert plot was obtained in the measured ground-state concentration range (0.05–1.0 mM).

Excitation of CPPT at 434 nm in acetonitrile leads to an emission spectrum with a maximum at 495 nm, Fig. 3. The fluorescence emission band overlaps the fluorescence excitation (or absorption) band showing a normal Stokes shift.

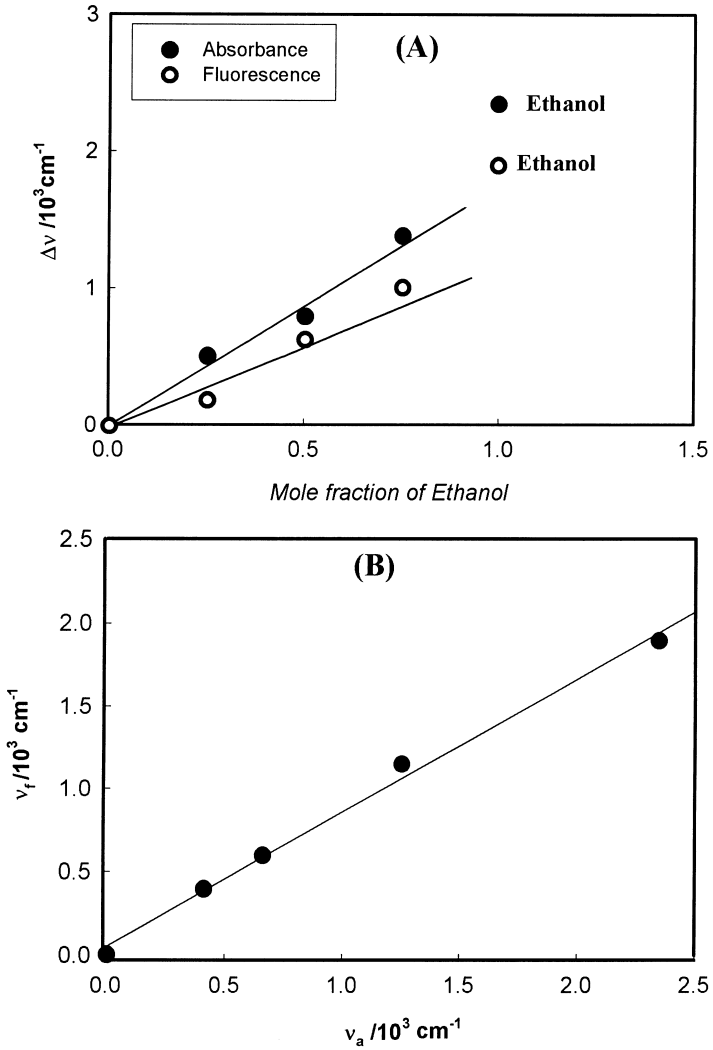

Fig. 2. (A) Plot of the relative fluorescence and absorption shifts, Δv, for CPPT vs. mole fraction of ethanol in CCl_4 and (B) plot of the relative fluorescence shift, v_f, vs. the relative absorption shift, v_a, for CPPT at different ethanol/CCl_4 composition.

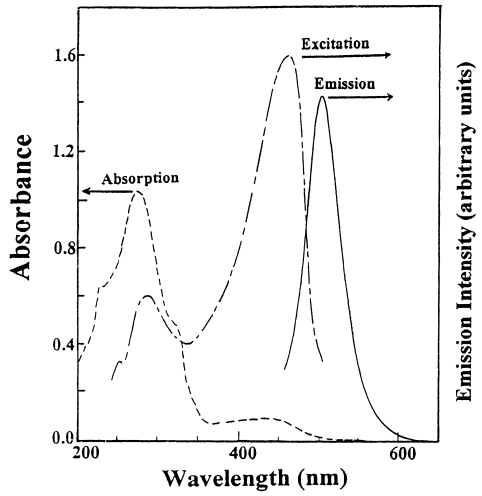

Fig. 3. (A) Absorption (---), fluorescence at $\lambda_{ex} = 434$ nm (–) and fluorescence excitation spectra (––) at 500 nm of CPPT (5×10^{-5} M) in acetonitrile.

The data in Table 1 show that the fluorescence maxima for CPPT (or CPPSH) and CMPT (or CMPSH). The fluorescence maxima generally display blue shift with increasing the polarity of alcoholic solvents and with increasing the polarity of polar aprotic solvents (CH_3CN and DMF). The shifts of the fluorescence peak are almost parallel to those of absorption maxima. The Stokes shifts shown in Table 1 in non polar solvents are slightly small than those in polar solvents.

Shifts of the absorption and fluorescence spectra of CPPT (or CMPT) can be analyzed in relation to solvatochromic scales introduced by Biolet–Kawaski (BK) [35]. Fig. 4A shows the absorption and fluorescence maxima of CPPT in various solvents as a function of BK. The linear dependence of the maximum absorption is parallel to that of the maximum fluorescence (ethanol deviate from the straight line). The dependence of the maximum fluorescence, v_f, on the maximum absorption, v_a, of CCPT shows a good linearity with slope equal to 0.81 and correlation coefficients equal to 0.960 (Fig. 4B). This argument demonstrates that there is negligibly small difference between the ground and excited states geometry and also suggests that similar prototropic equilibria occur in the ground and excited states.

3.2. Transient absorption spectra

In Ar-saturated ethanol, time-dependent transient absorption spectra observed by the 266 nm laser excitation of CPPT are shown in Fig. 5. The spectrum immediately after the laser excitation has maxima at 370 and 530 nm. Similar behavior was obtained for CMPT. The transients decayed quickly within 2.5 μs (Fig. 5). The decay rates of the both transient bands were effectively accelerated by addition of O_2 into the solution, suggesting that the both transient bands are due to the triplet–triplet (T–T) transition of ^{3}(CPPT)* and ^{3}(CMPT)*. ^{3}(CPPT)* and ^{3}(CMPT)* are formed from the

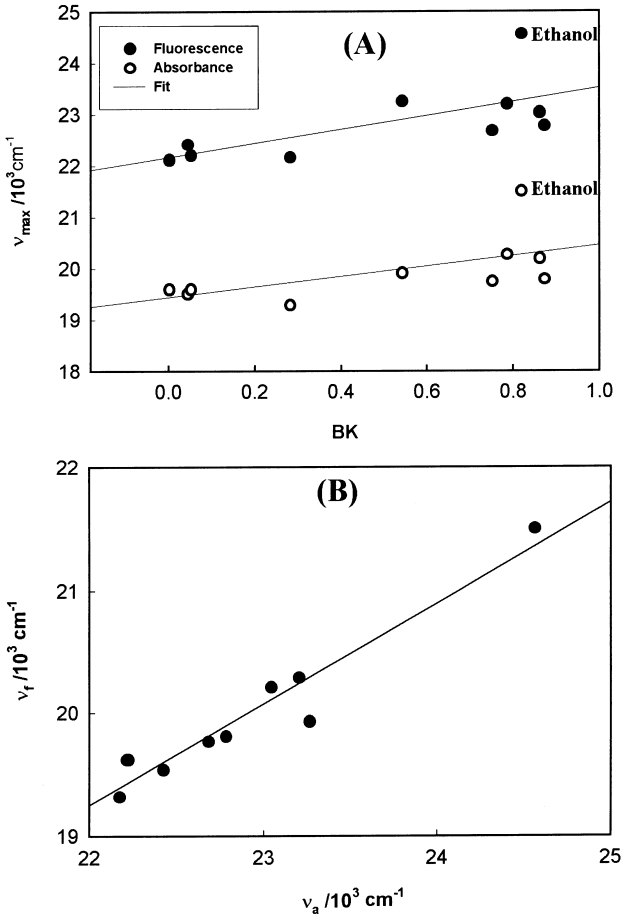

Fig. 4. (A) Fluorescence and absorption maximum in wavenumber for the CPPT as a function of BK and (B) plot of the fluorescence maximum vs. absorption maximum for CPPT in various solvents.

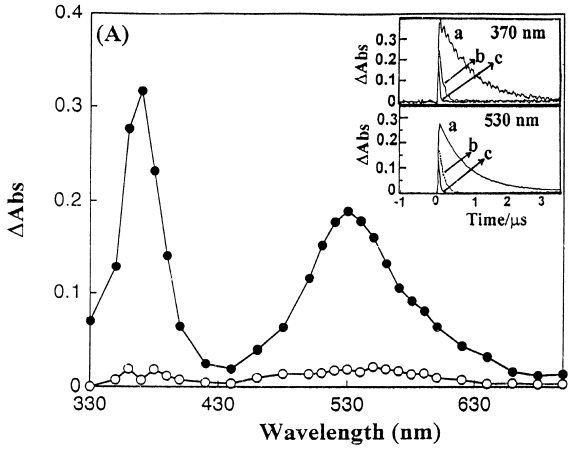

Fig. 5. Transient spectra recorded by laser photolysis of CPPT (1.0×10^{-4} M) with 266 nm light: (●) 0.25 μs and (O) 2.5 μs, in Ar-saturated ethanol. Inset: decay profiles, in (a) Ar-saturated; (b) air-saturated and (c) O_2-saturation.

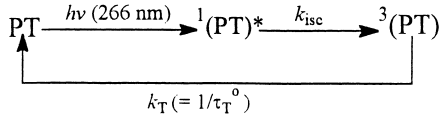

Scheme 2.

excited singlet states via intersystem crossing as shown in Scheme 2.

Each decay curve obeys the first-order kinetics in the absence and presence of O_2, from which the first-order rate constant was evaluated (k_{1st}) as shown in the inset of Fig. 5. The k_{1st} value increases with the O_2-concentration; the pseudo-first-order plot gives the second-order rate constant (k_{O_2}) for the quenching reaction of ^{3}(PT)* with O_2; they are summarized in Table 2.

$$^3(PT)^* \xrightarrow{k_{O_2}} PT + {}^1O_2^* \quad (1)$$

The formation of singlet oxygen $^1O_2^*$ was confirmed by consumption of 1,3-diphenylisobenzofuran [36]. The oxygen quenching of ^{3}(CPPT)* in ethanol is efficient and occurs with rate constant ($k_{O_2} = 1.65 \times 10^9\ M^{-1}\ s^{-1}$) close to 3/10 k_{diff}. In the case of ^{3}(CMPT)*, the $k_{O_2} = 3.28 \times 10^9\ M^{-1}\ s^{-1}$ in ethanol which is close to 6/10 k_{diff}, where k_{diff} is the rate constant for diffusion controlled limit ($k_{diff} = 5.6 \times 10^9\ M^{-1}\ s^{-1}$ in ethanol). The k_{diff} value was calculated from Debye–Smoluckowski equation ($k_{diff} = 8RT/3000\eta$) [37].

In CCl_4, the transient absorption spectra observed by the laser excitation of CPPT (or CPPSH) are shown in Fig. 6A, which are quite different from those in ethanol. The broad transient absorption band was observed in the visible region with peak around 430 nm. The decay rate in Ar-saturated solution was quite slow compared with that of ^{3}(CPPT)* in Fig. 5. In the presence of O_2, the decay rates were also accelerated. However, the decay rates were slower than those of ^{3}(PT)* in Fig. 5. This suggests that the transient species produced by the photolysis in CCl_4 and cyclohexane are thio radicals generated by a photoinduced homolytic S–H bond cleavage of CPPSH [38–40] as in Eq. (2).

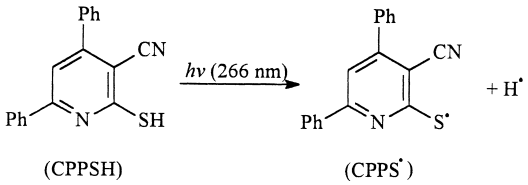

(2)

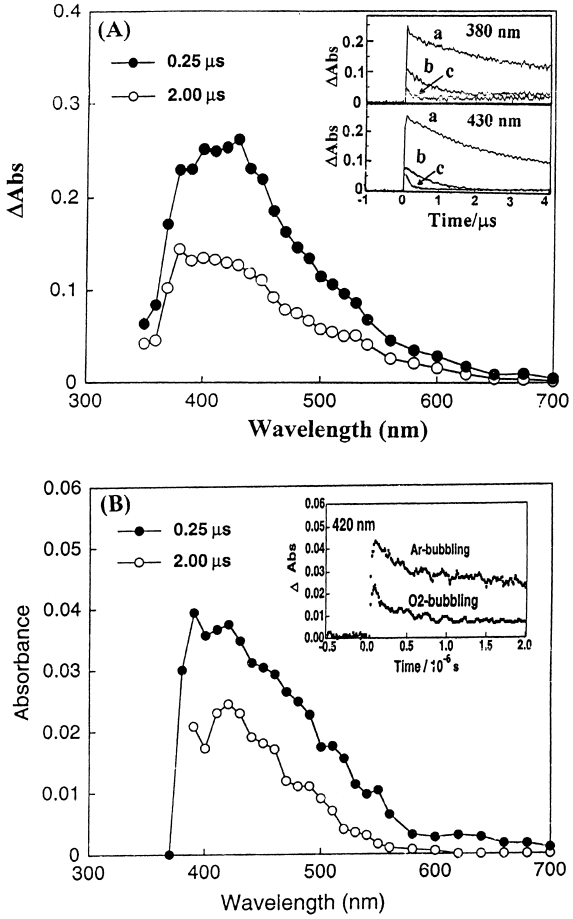

Fig. 6. Transient absorption spectra observed by laser photolysis with 266 nm light in Ar-saturated CCl_4, (A) CPPT (1×10^{-4} M). Inset: decay-time profiles in (a) Ar-saturated; (b) air-saturated, and (c) O_2-saturated solutions. (B) Disulfide of CPPT (1×10^{-4} M). Inset: decay-time profiles.

In Fig. 5B, the transient spectra observed by the laser excitation of the disulfide of CPPT (CPPS–SPPC) in CCl_4 are shown. The transient spectra are quite similar to those from CPPT (or CPPSH). From the photolysis of the disulfide, most probably transient species is the thio radical (CPPS$^\bullet$), formed by homolytic photodissociation at the S–S bond of CPPS–SPPC according to Eq. (3). In general, the thio radical is insensitive to O_2, the decay rate of the thio radical was accelerated in the presence of O_2. The presence of an acceptor group (–CN) in the *ortho* position of the thio

Table 2
Triplet state properties of CPPT and CMPT in various solvents at 298 K[a]

Data	CPPT			CMPT		
	Ethanol	CH_3CN	CCl_4	Ethanol	CH_3CN	CCl_4
k_{O_2} ($M^{-1}\ s^{-1}$)	1.65×10^9	1.49×10^9	2.66×10^8	3.28×10^9	2.10×10^9	3.8×10^8
k_{sq} ($M^{-1}\ s^{-1}$)	3.60×10^{10}	5.68×10^9		2.70×10^{10}	2.99×10^9	
τ_T^0 (μs)	1.84	3.70		0.90	2.91	

[a] The intrinsic lifetime (τ_T^0) was estimated by extrapolation to infinite dilution in the plots of $k_{obs}(1/\tau_T)$ vs. [PT] for ^{3}(CPPT)* or ^{3}(CMPT)*, respectively.

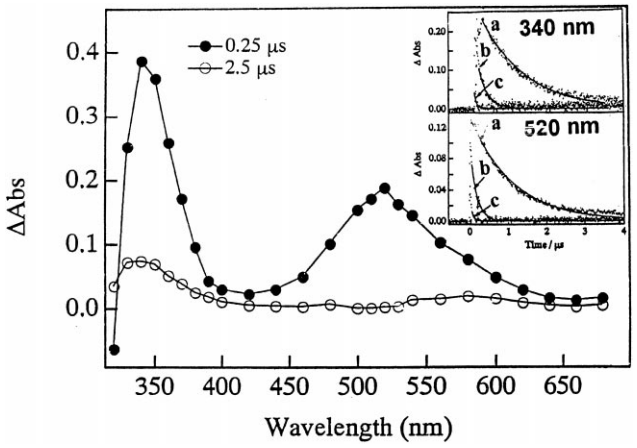

Fig. 7. Transient absorption spectra observed after laser photolysis of CPPT (1.0×10^{-4} M) with 266 nm light in Ar-saturated acetonitrile. Inset: decay-time profiles in (a) Ar-saturated, (b) air-saturated, and (c) O_2-saturated solutions.

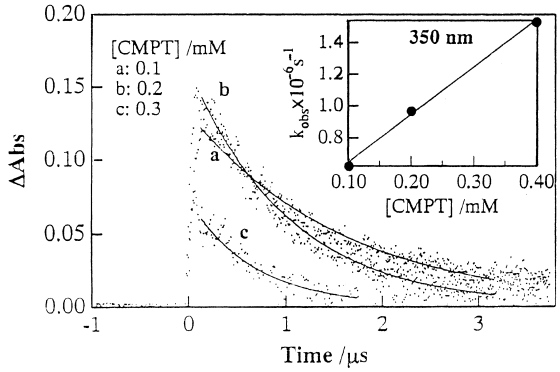

Fig. 8. Self-quenching of ^{3}(CMPT)* at 350 nm in Ar-saturated acetonitrile. Inset shows pseudo first-order-plot.

radical group may be responsible for the reactivity of the thio radical to O_2.

$$\text{CPPS–SPPC} \overset{h\nu(355\,\text{nm})}{\rightarrow} 2\text{CPPS}^{\bullet} \quad (3)$$

In acetonitrile, which shows the intermediate shifts of absorption and fluorescence peaks (Table 1), the transient absorption bands observed by the laser excitation of CPPT are shown in Fig. 7. The transient absorption bands at 520 and 350 nm are quite similar to those in ethanol. Thus, they are attributed to ^{3}(CPPT)*. Similar transient spectra were observed for CMPT in other polar solvents such as dimethylformamide and ethyl acetate, indicating that CPPT and CMPT in intermediate solvents such as dimethylformamide and ethyl acetate are predominantly present as thione-form.

The k_{O_2} value evaluated for ^{3}(CPPT)* in acetonitrile ($1.49 \times 10^9\,M^{-1}\,s^{-1}$) is also quite similar to that in ethanol ($1.65 \times 10^9\,M^{-1}\,s^{-1}$), which is a typical solvent for thione-form. The k_{O_2} value is approximately six times larger than that of the thio radical ($2.66 \times 10^8\,M^{-1}\,s^{-1}$) in CCl_4. In deaerated acetonitirle, the decay rates depend on the CPPT concentration as shown in Fig. 8. The decay rates ($k_T = 1/\tau_T$) increase with the ground-state concentration of CPPT, which indicates the self-quenching (k_{sq}) takes place according to Eq. (4). The self-quenching rate constant (k_{sq}) and the triplet lifetime (τ_T^0), which are defined as intrinsic, can be evaluated from the slope and the intercept of linear plot, based on Eq. (5), as shown in the insert of Fig. 8. The k_{sq} value for CMPT was evaluated as to be $2.99 \times 10^9\,mol^{-1}\,dm^3\,s^{-1}$. For CPPT, the k_{sq} value of $5.68 \times 10^9\,mol^{-1}\,dm^3\,s^{-1}$ was estimated. Such large k_{sq} and relatively short lifetime values are typical characteristics of thione triplets [4,9]. The estimated data are listed in Table 3.

$$^3(\text{PT})^* + \text{PT} \overset{k_{sq}}{\rightarrow} \text{PT} + \text{PT} \quad (4)$$

$$\frac{1}{\tau_T} = \frac{1}{\tau_T^0} + k_{sq}[\text{PT}] \quad (5)$$

3.3. Steady-state photolysis

Steady-state photolysis of CPPSH and CMPSH in non-polar solvents produced the corresponding disulfide as shown in Fig. 9A. The absorption band in the longest wavelength (450 nm) was decreased with irradiation time, accompanying with the increase in the absorption band at 335 nm, although it seems to be the shift of the band at 300 nm of CPPSH. The final spectrum of CPPSH was similar to that of pure disulfide in the same solvent (inset of Fig. 9A).

In acetonitrile (Fig. 9B) the decrease of the absorption band of CPPT at 434 nm was quite slow, indicating that the conversion from the thione to the corresponding disulfide is slow process. The final formation of the disulfide in acetonitirle suggests that the low tautomeric equilibrium concentration of the thiol-form is photodissociated to give the disulfide slowly (inset in Fig. 9B). In ethanol, the decrease of the absorption band of CPPT at 407 nm was quite slow,

Table 3
Solvent effects on the fluorescence characteristics of CMPT at 298 K

Solvent	τ (ns) (amplitude, A)		Φ_f	$k_r \times (10^6\,s^{-1})$	$k_{nr} \times (10^8\,s^{-1})$
	τ_1 (A_1%)	τ_2 (A_2%)			
Acetonitrile	6.33 (71.02)	1.48 (28.98)	0.036	5.19	0.99
Ethanol	6.03 (74.04)	1.26 (25.96)	0.026	4.31	1.61
CCl_4	–	1.22 (100)	0.021	17.21	8.02

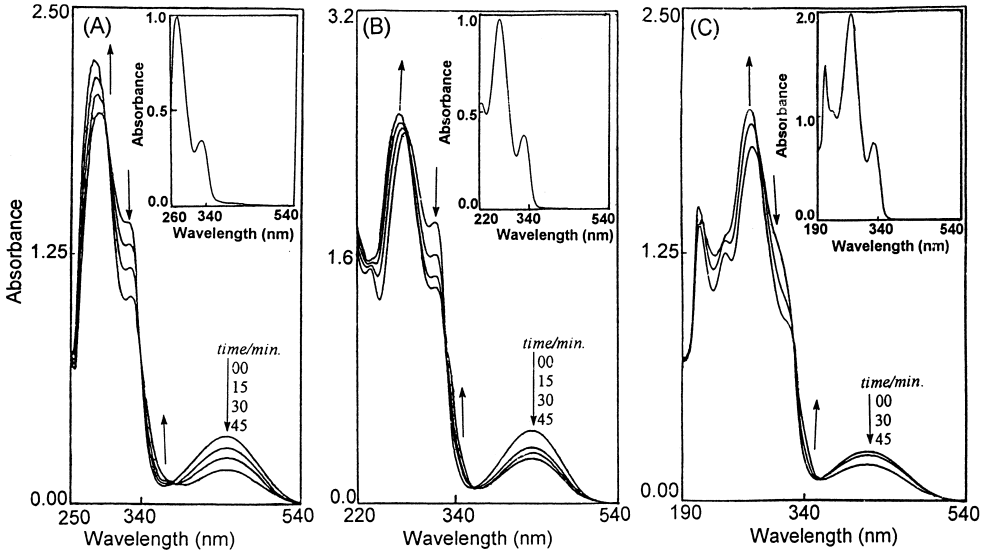

Fig. 9. (A) Steady-state photolysis of CPPT (8.3×10^{-5} M) with light longer than 330 nm and optical path of 1 cm in: (A) CCl_4; (B) acetonitrile and (C) ethanol. The inset show the absorption spectra of disulfide CPPS-SPPC.

indicating that contribution of the thiol-form to the tautomeic is low (Fig. 9C).

An evidence for these conclusions is the observed rate constant value for thiol-disulfide transformation in CCl_4 is $2.78 \times 10^{-4}\,s^{-1}$. This value is larger than the corresponding rate constants for thione-disulfide in acetonitrile ($1.86 \times 10^{-4}\,s^{-1}$) and ethanol ($1.44 \times 10^{-4}\,s^{-1}$). The trend of increasing the efficiency of the steady state photolysis is consistent with the solvent shift of the longer absorption wavelength.

3.3.1. Fluorescence lifetime and quantum yield

The fluorescence decay times of CMPT are determined in three different solvents: ethanol, acetonitrile, and CCl_4 (Table 3). Fig. 10 shows the representative fluorescence decay data of CMPT in ethanol. Improvement in the value of chi-squared and the distribution of residuals was observed when going from a single to a double exponential fit in ethanol and acetonitrile, suggesting the existence of different fluorescent species. The lifetime values (Table 3) are calculated using the expression

$$I(t) = \sum_{i=1}^{n} A_i \exp\left(\frac{-t}{\tau_i}\right) \tag{6}$$

where $I(t)$ is the intensity of the fluorescence at time t, A_i the pre-exponential factor for the fraction of the fluorescence intensity, τ_i the fluorescence lifetime of the emitting species and n the total number of emitting species.

Table 3 provides representative data that illustrate the sensitivity of both fluorescence quantum yields Φ_f and lifetimes τ_1 and τ_2 to the nature of the solvent. As can be seen from Table 3, there is a slight decrease of Φ_f in going from protic (ethanol) and polar aprotic (acetonitrile) media to less polar solvents such as CCl_4. A more prominent difference was observed in the lifetime τ_1 of the major process; in ethanol and acetonitrile, the lifetimes of the major process (6.03–6.33 ns) are quite longer than that in CCl_4 (1.22 ns). Also, the shorter value (τ_2) in ethanol and acetonitrile is

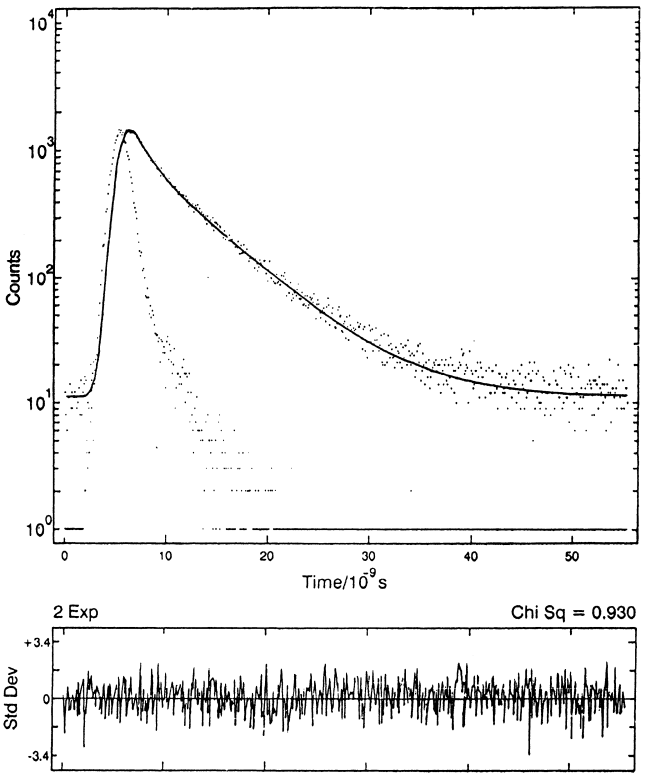

Fig. 10. Excitation pulse profile, fluorescence decay and residuals plots of CMPT in ethanol. The excitation and emission wavelengths are 400 and 462 nm, respectively.

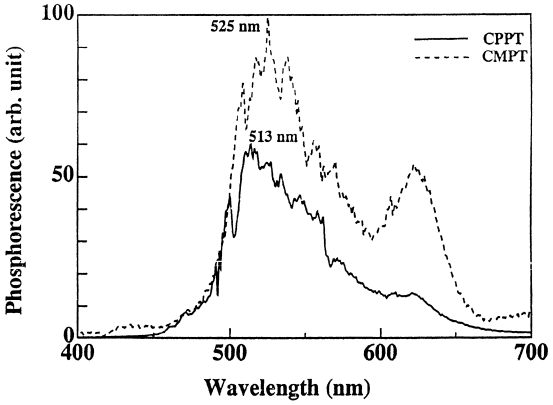

Fig. 11. Phosphorescence spectra observed for CPPT and CMPT at 77 K in glassy ethanol.

close to those reported in CCl_4. Hence, the longer lifetime (≈6 ns) can be assigned to the thione form and the shorter lifetime (≈1 ns) is due to the thiol form.

The radiative and nonradiative rate constants have been calculated from $k_r = \Phi_f/\tau_f$ and $k_{nr} = (1-\Phi_f)/\tau_f$, respectively. In ethanol and acetonitrile, the k_{nr} values are found to be about 17–37 times faster than the radiative rate k_r, in accordance with the considerably large intersystem crossing for thiones [4,6]. In CCl_4, the k_{nr} value is five to eight times larger than those for thione-form; the k_r value is three time larger than those for thione-form. This also supports the predominant presence of the thiol-form.

3.4. Phosphorescence emission

Fig. 11 shows the phosphorescence spectra of CPPT and CMPT at 77 K ($\lambda_{ex} = 320$ nm) in ethanol. The phosphorescence bands were observed at 525 and 620 nm for ^{3}(CMPT)*, where the phosphorescence bands of ^{3}(CPPT)* were observed at 513 and 620 nm. The triplet energies (E_{T1}) were estimated from the first phosphorescence peak to be 55.74 and 54.45 kcal/mol for ^{3}(CPPT)* and ^{3}(CMPT)*, respectively. The peak at 620 nm may be considered as double of the excitation wavelength. In other solvents, the measurements of the phosphorescence spectra were difficult, because of poor transparency.

4. Conclusions

The strong solvent dependence of the tautomeric equilibrium of CPPT and CMPT and the distinct absorption properties of their thione and thiol forms allow the investigation of the photochemistry of each tautomer. In nonpolar and less polar solvents, laser flash photolysis of CPPSH and CMPSH predominantly generate the thio radicals CPPS· and CMPS, respectively, by homolytic fission of the S–H bond. The thiol forms CPPSH and CMPSH gave relatively fast steady-state photolysis to the corresponding disulfide CPPS–SPPC and CMPS–SPMC.

In polar and protic solvents, the photochemical behavior of the thione tautomer exhibiting properties such as slow steady state photolysis to the corresponding disulfide, Their triplet states ^{3}(CPPT)* and ^{3}(CMPT)* exhibiting short lifetime and efficient self quenching by the ground-state. However, the excited-singlet state lifetime of the thiol ^{1}(CMPSH)* is far shorter than that of the corresponding thione tautomer ^{1}(CMPT)*.

Acknowledgements

One of authors (O. Ito) would like to express his thanks to the supports from the Ministry of Education, Science, Sports, and Culture, Japan (the Grant-in Aid on Scientific Research on Priority Area (B) on “Laser Chemistry of Single Nanometer Organic Particle” (No. 10207202)).

References

[1] A. Albert, G. Barlin, J. Chem. Soc. (1959) 2384.
[2] J. Wirtz, J. Chem. Soc. Perkin 2 (1973) 1307.
[3] C.V. Kumar, L. Qin, P.K. Das, J. Chem. Soc., Faraday Trans. 2 80 (1984) 783.
[4] A. Maciejewski, D.R. Demmer, D.R. James, A. Safarzadeh-Amiri, R.E. Verrall, R.P. Steer, J. Am. Chem. Soc. 107 (1985) 2831.
[5] K. Bhattachayya, V. Ramamurthy, P.K. Das, J. Phys. Chem. 91 (1987) 5626.
[6] A. Maciejewski, M. Syzmamurthy, R.P. Steer, J. Phys. Chem. 92 (1988) 6939.
[7] R. Minto, S. Samanta, P.K. Das, Can. J. Chem. 67 (1989) 967.
[8] J. Kamphuis, H.J.T. Bos, R.J. Visser, B.H. Huizer, C.A. Varma, J. Chem. Soc., Perkin Trans. 2 (1986) 1867.
[9] M. Alam, M. Fujitsuka, A. Watanabe, O. Ito, J. Chem. Soc., Perkin Trans. 2 (1998) 817.
[10] E. Shaw, J. Bernstein, K. Loser, W.A. Lott, J. Am. Chem. Soc. 72 (1950) 4362.
[11] A. Albert, Selective Toxicity: The Physico-Chemical Basis of Therapy, 7th Edition, Chapman & Hall, London, 1985.
[12] J. Konotoghiorghes, A. Piga, A.V. Hoffbrand, Hematolog. Oncol. (1986) 195.
[13] W. Adam, J. Cadet, F. Dall’Acqua, D. Ramaiah, C.R. Saha-Moller, Angew. Chim. 107 (1995) 91.
[14] M. Alam, M. Fujitsuka, A. Watanabe, O. Ito, J. Phys. Chem. 102 (1998) 1338.
[15] M. Alam, M. Fujitsuka, A. Watanabe, O. Ito, Photochem. Photobiol. 63 (1996) 53.
[16] W. Adam, D. Ballnier, B. Epe, G.N. Grimm, C.R. Saha-Moller, Angew. Chim. Int. Ed. Engl. 34 (1995) 2156.
[17] B. Epe, D. Ballmaier, W. Adam, G.N. Grimn, C.R. Saha-Moller, Nucl. Acids Res. 24 (1996) 1625.
[18] A.J.S.C. Vieira, J.P. Telo, R.M.B. Dias, J. Chim. Phys. 94 (1997) 318.
[19] S. Stoyanov, T. Stoyanova, L. Antonov, P. Karagiannidis, P. Akrivos, Monatsheft für Chem. 127 (1996) 495.
[20] A. Katrizky, J. Lagowski, Adv. Heterocycl. Chem. 1 (1963) 312.
[21] P. Beak, J. Convington, S. Smith, J. Am. Soc. 98 (1976) 8284.
[22] P. Beak, J. Convington, S. Smith, J. White, J. Zeiger, J. Org. Chem. 54 (1980) 1354.
[23] M. Rubio, C. Seoane, J. Soto, Heterocyclic 20 (1983) 783.

[24] A. Les, L. Adamowicz, J. Phys. Chem. 94 (1990) 7021.
[25] A.O. Colson, B. Bester, M.D. Sevilla, J. Phys. Chem. 96 (1992) 9787.
[26] M.J. Stewart, J. Leszczynski, Y.V. Rubin, Y.P. Blagoi, J. Phys. Chem. A 101 (1997) 4753.
[27] A. Broo, J. Phys. Chem. A 102 (1998) 526.
[28] M. Orozco, B. Hernandez, F.J. Luque, J. Phys. Chem. B 102 (1998) 5228.
[29] G. El Gemeie, A. El Zanate, A. Mansour, J. Chem. Soc., Perkin. Trans. 1 (1992) 1073.
[30] S. Stoyanov, I. Petkov, L. Stoyanova, T. Antonov, P. Karagiannidis, P. Aslanidis, Can. J. Chem. 68 (1990) 1482.
[31] M. El-Kemary, Can. J. Anal. Sci. Appl. Spectrosc. 43 (1998) 95.
[32] M. El-Kemary, M. Fujitsuka, O. Ito, J. Phys. Chem. A 103 (1999) 1329.
[33] R.A. Jones, A.R. Katritzkey, J. Chem. Soc. (1960) 2937.
[34] B.M. Avelines, I.E. Kochevar, R.W. Redmond, J. Am. Chem. Soc. 118 (1996) 10113.
[35] L. Bilot, A. Kawaski, Z. Naturforsch. A 17 (1962) 621.
[36] H.H. Wasserman, R.W. Murray, Singlet Oxygen, Academic Press, New York, 1979 (Chapters 5, 6, 8 and 9).
[37] K.U. Ingold, in: J.K. Koch (Ed.), Free Radicals, Wiley, New York, 1973, p. 37.
[38] M. Alam, O. Ito, J. Org. Chem. 64 (1999) 1285.
[39] W.A. Pryor, E.G. Olsen, J. Am. Chem. Soc. 100 (1978) 2852.
[40] O. Ito, M. Matsuda, J. Am. Chem. Soc. 101 (1979) 1815.